

UNCLASSIFIED

Defense Technical Information Center
Compilation Part Notice

ADP012248

TITLE: Soft Reverse Current-Voltage Characteristics in V2O5 Nanofiber Junctions

DISTRIBUTION: Approved for public release, distribution unlimited

This paper is part of the following report:

TITLE: Nanophase and Nanocomposite Materials IV held in Boston, Massachusetts on November 26-29, 2001

To order the complete compilation report, use: ADA401575

The component part is provided here to allow users access to individually authored sections of proceedings, annals, symposia, etc. However, the component should be considered within the context of the overall compilation report and not as a stand-alone technical report.

The following component part numbers comprise the compilation report:

ADP012174 thru ADP012259

UNCLASSIFIED

Soft reverse current-voltage characteristics in V_2O_5 nanofiber junctions

Gyu-Tae Kim, Jörg Muster, Marko Burghard, and Siegmur Roth

Max-Planck Institut für Festkörperforschung, Heisenbergstr. 1, D-70569, Stuttgart, Germany

ABSTRACT

V_2O_5 nanofibers showed the rectifying current-voltage characteristics under an asymmetric contact configuration at room temperature, indicating the formation of a Schottky diode. The ideality factors as a Schottky diode were estimated to be 6.1 at the forward bias and 1.4 at the reverse bias. The larger current at the reverse bias defined by the negative voltage at the metal electrode may originate from the contribution of the tunneling via field emission or thermionic field emission. The ultimate geometric size of nanofibers enhances the influence of the tunneling mechanism and modifies the nano-scale Schottky diode, requiring more understanding in designing the nano-scale electronic devices with the metal contacts.

INTRODUCTION

Synthetic nanofibers such as carbon nanotubes are invoking the scientific interest nowadays [1-3]. With the development of the synthesis techniques for the synthetic nanofibers, the molecular electronics based on synthetic nanofibers become more plausible by making the nano-scale electronic devices [2-7]. To achieve the realistic electronic chips, all practical issues such as electrical connection, the assembling technique and the integration processes should be considered for the new functional nano-scale devices [4,7]. Till now the electrical properties of nanofibers were investigated from the point of a field effect transistor, a rectifying diode and optoelectronic devices [3-7]. As the carbon nanotube is under the highlight because of its noble structure and outstanding electrical properties, other synthetic nanofibers are also attracting from the basic research and the application [2,3,6,7]. V_2O_5 nanofiber was found a century ago, and identified to have the ultimate geometric dimension with a good uniformity in the fibrous structure [8]. Recently a field effect transistor made of V_2O_5 nanofibers was demonstrated with a small electrical mobility of 10^{-2} $\text{cm}^2/\text{V s}$ owing to the hopping conduction [6]. Most of the electrical contacts defined on the V_2O_5 nanofibers showed the ohmic behaviors, indicating the symmetric contact in the two-probe configuration [9]. In the present study, a significant asymmetric current-voltage characteristics in a V_2O_5 nanofiber junction is shown and discussed by considering the influence of the tunneling mechanism through the nanofiber Schottky barrier.

EXPERIMENT

V_2O_5 sols were prepared from 0.2 g ammonium(meta)vanadate (NH_4VO_3) and 2 g acid ion exchange resin (DOWEX 10x80) in 40 ml water. With aging for a few days, the average length of floating individual V_2O_5 nanofibers in the orange color solution increases up to a few μm . For the better deposition of individual V_2O_5 nanofibers on bare substrates, a Si substrate silanized by 3-aminopropyltriethoxysilane (3-APS) solution was dipped into a mixture of V_2O_5 sol/water (1:10) for 2 ~ 3 sec. Afterwards, the substrate was rinsed with water, and blown dry. Au/Pd (40%/60%) lines with a separation of 100 nm were defined on the substrate by e-beam

lithography using a two-layer resist and a modified Hitachi S2300 scanning electron microscope. Current-voltage characteristics were recorded under the low pressure of Helium atmosphere with a Keithley 617 electrometer and a Keithley 230 voltage source.

RESULTS & DISCUSSION

Figure 1 (a) shows a scanning force microscope (SFM) image of the V_2O_5 nanofibers under the Au/Pd electrodes patterned by e-beam lithography. The number of the individual V_2O_5 nanofibers under the electrodes is 8. The V_2O_5 nanofibers are long enough to reach among the four successive electrodes. In Figure 1 (b), the current-voltage characteristics among the different electrode pairs are recorded at room temperature. All the two-probe pairs without the electrode 1 showed ohmic behaviors in the range of the resistance about $50\text{ M}\Omega$. All the pairs with the electrode 1 showed the gap feature indicating the existence of the asymmetric contact barriers at the contact 1. By the charge transfer between metal electrode and n-type V_2O_5 nanofibers, a Schottky barrier could be formed at the contact 1 as a depletion layer [6,10-12]. The turn-on voltages at the negative bias on the electrode 1 are lower than those at the positive bias, indicating the p-type carrier in the V_2O_5 nanofiber. Considering the n-type carrier in V_2O_5 nanofibers [6,10,11], the polarity of the forward bias contradicts, so-called soft-reverse characteristics [12,13,16,17].

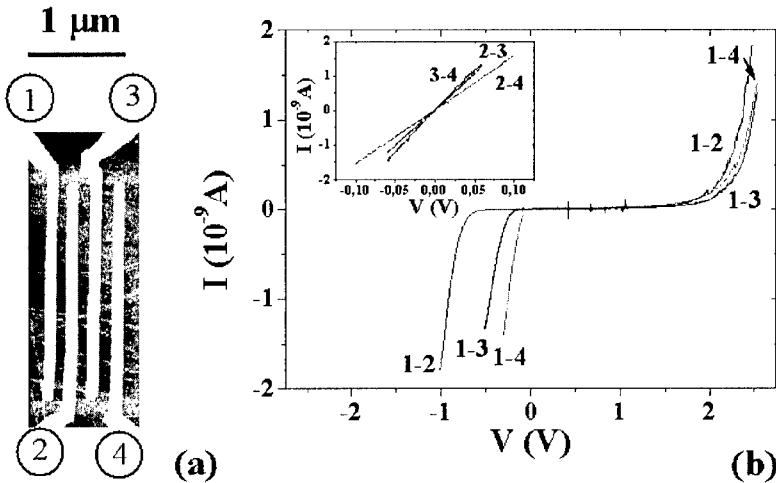


Figure 1. (a) Scanning force microscope image of V_2O_5 nanofibers below the Au/Pd electrodes with the neighboring distance, 100 nm. (b) Current-Voltage characteristics of each electrode pair at room temperature. „n-m“ convention denotes the positive polarity at the electrode „n“ and the negative polarity at the electrode „m“. All electrode pairs including the electrode 1 show the rectifying behaviors with the asymmetric tendencies. The inset indicates the ohmic properties of the electrode pairs without the electrode 1.

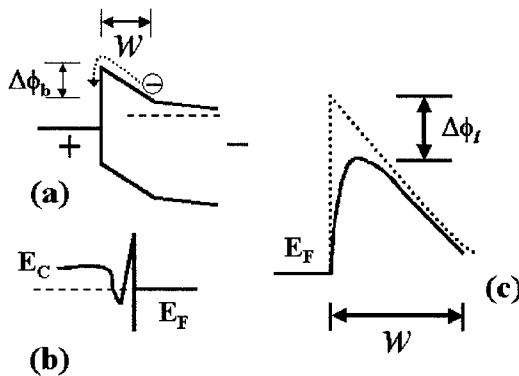


Figure 2. (a) Band configuration for the forward bias in a metal-n type semiconductor junction. $\Delta\phi_b$ indicates the barrier height at the normal forward bias configuration. (b) Local doping can induce a shallow tunneling barriers, resulting in an ohmic behavior. (d) Barrier lowering factors ($\Delta\phi_l$) can increase the current at the reverse bias.

By the the chemical potential alignment between the metal electrode and an n-type semiconductor as shown in Figure 2 (a), the forward bias can be defined as the positive voltage at the metal electrode [12,13]. With the negative bias at the semiconducting V_2O_5 nanofiber, the energy barrier ($\Delta\phi_b$) decreases because the energy of the conduction band rises. But this insight fails to explain the larger current at the negative polarity shown in Figure 1 (b). Interestingly, in the case of a carbon nanotube Schottky diode, a similar reversal behavior can be found in literature [14]. The contact barrier at the electrode 1 may lie along the surface of the V_2O_5 nanofibers below the electrode in a vertical configuration. The tiny pin-hole or the local doping can increase the leakage current in a V_2O_5 nanofiber junction as in Figure 2 (b) by the increased tunneling current, giving an ohmic behavior. The finite thickness of the V_2O_5 nanofiber can limit the widening or shrinking of the junction width which is different from the bulk case. According to the recent theoretical studies on the nanofiber Schottky junctions, the heavy doping can decrease the barrier width in a very narrow layer [15]. The fact that the most contacts showed the ohmic behaviors at room temperature possibly indicates the existence of a heavily doped layer as a short tunneling path. As the temperature decreases, the ohmic behavior changed to the slight non-ohmic curves but still with a symmetric tendency, indicating the existence of the symmetric thin contact barriers at the electrodes. At room temperature the ohmic transport through most of the electrodes can make it possible to assume negligible contact barriers at the electrodes except the electrode 1, which also enables the determination of the right polarity of the forward bias at the asymmetric contact barrier, the electrode 1. In the reverse bias, the equivalent circuit can be modeled by the combination of resistors and diode components as in the inset of Figure 3. Following a detailed circuit analysis, the bulk resistances in the equivalent circuit could be estimated as following ; $R_2= 64.2 \text{ M}\Omega$, $R_3= 53.0 \text{ M}\Omega$, $R_{23}= 140.5 \text{ M}\Omega$. According to the conventional Schottky diode, the current can be analyzed by the relation of the current, $i = i_0[\exp(qV / \eta k_B T) - 1]$, where η is ideality factor in Schottky barrier [12,13].

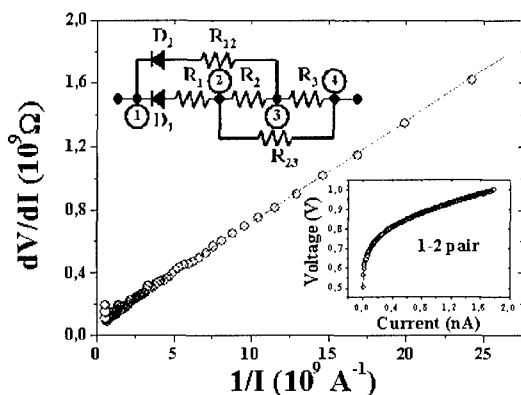


Figure 3. The equivalent circuit of the V_2O_5 nanofibers corresponding to Figure 1. At the electrode 1, the two diode components are assumed in the reverse bias configuration. The dashed lines indicate the best fitting following equation (1) and (2).

$$V = iR + \frac{\eta k_B T}{q} \ln\left(\frac{I}{I_0}\right) \quad (1)$$

$$\frac{dV}{dI} = R + \frac{\eta k_B T}{qI} \quad (2)$$

From the relation of the equation (1) and (2), the linear relationship between dV/dI and $1/I$ can be deduced and Figure 3 shows a good agreement. By the same procedures with the different electrode pairs, R_1 and R_{12} could be determined as $R_1 = 70.9 \text{ M}\Omega$ and $R_{12} = 132.1 \text{ M}\Omega$. Two diode components were resolved as $I_{D1} = 2.31 \times 10^{-15} \exp(V/0.06435)$ and $I_{D2} = 1.71 \times 10^{-13} \exp(V/0.03636)$ with the ideality factors $\eta_1 = 2.55$ and $\eta_2 = 1.44$ in the reverse configuration. The prefactor of the current is given by the relation of $I_0 = A^{**} S T^2 \exp(-q \Delta\phi_b / k_B T)$ where A^{**} is the effective Richardson constant and S the area of the junction [12,13]. The barrier heights $\Delta\phi_b$ were calculated to be 0.57 eV for D_1 and 0.46 eV for D_2 with an assumption of the junction area as $8 \times 1.5 \text{ nm} \times 100 \text{ nm}$. If the junction area is assumed as the cross-section of the V_2O_5 nanofibers, $8 \times 1.5 \text{ nm} \times 10 \text{ nm}$, the barrier heights are calculated to be 0.51 eV for D_1 and 0.40 eV for D_2 . So the barrier height can be guessed between 0.4 eV and 0.6 eV, which is quite in the range of the energy gap of V_2O_5 nanofibers, $E_g = 2.2 \text{ eV}$ [8-11]. Following the similar analysis, the ideality factors of D_1 and D_2 were estimated to be about 6.1 at forward bias which is quite larger than those at the reverse bias.

To explain the contradiction in the polarity of the apparent forward bias and the big differences in the ideality factors at the different bias, the tunneling contribution was considered as an origin of the soft-reverse characteristics. Assuming the high carrier concentration near the electrode contacts, the crowded electric field can enhance the tunneling probability of the carrier via the field emission or thermionic field emission [13,16,17]. These effects can be accentuated if the surface of V_2O_5 nanofiber is accumulated with the positive surface charges making the barrier at the edge even thinner. In the case of a gallium arsenide diode with a donor concentration of $2 \times 10^{18} \text{ cm}^{-3}$, the current at the reverse bias was known to exceed the current at the forward bias by field emission [17].

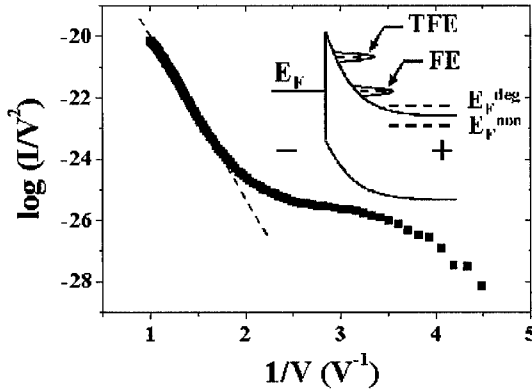


Figure 4. Fowler Nordheim tunneling model plot. The inset figure indicates the possible occurrence of the thermoionic field emission or the field emission in the Schottky barrier.

Figure 4 shows the Fowler-Nordheim tunneling plot, which fits rather well at high electric field [12]. From the calculation of the thermoionic field emission through a Schottky barrier, the current-voltage characteristics can be characterized as the equation (3), (4) and (5) [13].

$$J = J_s \exp(V_s / E_0) \quad (3)$$

$$E_0 = E_{00} \coth\left(\frac{qE_{00}}{k_B T}\right) \quad (4)$$

$$E_{00} = \frac{\hbar}{2} \left[\frac{N_d}{m^* \epsilon_s} \right]^{1/2} \quad (5)$$

Considering $N_d = \sigma / e \mu$ with $\sigma = 0.5$ (S/cm) and $\mu = 10^{-2}$ $\text{cm}^2/\text{V s}$ at room temperature [9], N_d can be estimated to be 3.1×10^{20} (cm^{-3}), which might be overestimated. E_{00} was estimated to be 0.143 eV and the ideality factor was estimated to be 5.7 from the value of E_0 , which is quite similar with our experimental ideality factor at the forward bias. Similarly, for the reverse direction in the tunneling regime, the current is given as following equation (6) and (7) [13]:

$$J = J_s \exp(V_r / E') \quad (6)$$

$$E' = E_{00} \left[\frac{qE_{00}}{k_B T} - \tanh\left(\frac{qE_{00}}{k_B T}\right) \right]^{-1} \quad (7).$$

So the ideality factor at the reverse bias can be estimated to be 1.21 from the value of E' , which is also quite similar with the value obtained in the measurement. So the consideration of the tunneling at the electrode 1 seems to be reasonable considering the ultra sharp shape of the metal electrode at the edge and the V_2O_5 thin nanofibers.

Large ideality factor was also reported in a carbon nanotube Schottky junction with a similar ideality factor, 5.8 [18]. Considering the restricted dimension, the junction property can be influenced much more than the bulk case by the enhanced electric field around the contact and

one dimensionality with the reduced screening [12]. More understanding on the physical properties of the electric contacts are still required.

SUMMARY

We observed the rectifying current-voltage characteristics in a metal-V₂O₅ nanofiber junction and the larger current at the reverse bias. The ideality factors at forward bias and reverse bias were explained by introducing the tunneling, which can give the soft reverse-current voltage characteristics.

ACKNOWLEDGMENTS

The authors are grateful to F. Schartner and U. Waizmann for technical support. G.T.K. would like to thank the support of Alexander von Humboldt Foundation. M. B. is grateful to the Deutsche Forschungsgemeinschaft (DFG) for financial support.

REFERENCES

1. R. Saito, G. Dresselhaus, and M. S. Dresselhaus, *Physical Properties of Carbon Nanotubes*, (Imperial College Press, London, 1998).
2. J.-C. P. Gabriel, and P. Davidson, *Adv. Mater.* **12**, 9 (2000).
3. X. F. Duan, and C. M. Lieber, *Adv. Mater.* **12**, 298 (2000).
4. W. B. Choi, J. U. Chu, K. S. Jeong, E. J. Bae, J.-W. Lee, J.-J. Kim, and J.-O. Lee, *Appl. Phys. Lett.* **22**, 3696 (2001).
5. S. J. Tans, A. R. M. Verschueren, and C. Dekker, *Nature*, **393**, 49 (1998).
6. G. T. Kim, J. Muster, V. Krstic, J. G. Park, Y. W. Park, S. Roth and M. Burghard, *Appl. Phys. Lett.* **76**, (2000)
7. X. Duan, Y. Huang, Y. Cui, J. Wang, and C. M. Lieber, *Nature*, **409**, 66 (2001).
8. T. Yao, Y. Oka, and N. Yamamoto, *Mat. Res. Bull.* **27**, 669 (1992).
9. J. Muster, G. T. Kim, V. Krstic, J. G. Park, Y. W. Park, S. Roth and M. Burghard, *Adv. Mater.* **12**, 420 (2000).
10. J. Livage, *Chem. Mater.* **3**, 526 (1991).
11. J. Bullot, O. Gallais, M. Gauthier, and J. Livage, *Appl. Phys. Lett.* **36**, 986 (1980).
12. S. M. Sze, *Semiconductor Devices and Physics and Technology* (Wiley, New York, 1985).
13. E. H. Rhoderick, *Metal-semiconductor contacts*, (Clarendon Press, Oxford, 1978).
14. Z. Yao, H. W. Ch. Postma, L. Balents, C. Dekker, *Nature*, **402**, 273 (1999).
15. F. Leonard, J. Tersoff, *Phys. Rev. Lett.* **83**, 5174 (1999).
16. A. Y. C. Yu, *Solid-St. Elect.* **13**, 239 (1970).
17. F. A. Padovani, *Semiconductors and semimetals* ed. by Willardson & Beer, **6A**, Chap. 2, (Academic Press, New York, 1971).
18. P. J. de Pablo, E. Graugnard, B. Walsh, R. P. Andres, S. Datta, R. Reifengerger, *Appl. Phys. Lett.* **74**, 323 (1999).